The Interaction of Shelf Accommodation, Sediment Supply and Sea Level in Controlling the Facies, Architecture and Sequence Stacking Patterns of the Tay and Forties/Sele Basin-Floor Fans, Central North Sea

David C. Jennette
Previous Address: ExxonMobil Upstream Research Company
P.O. Box 2189
Houston, Texas 77252-2189

Current Address: Bureau of Economic Geology
The University of Texas
University Station, Box X
Austin, Texas 78713-8924

Timothy R. Garfield
ExxonMobil Exploration Company
P.O. Box 4778
Houston, Texas 77210

David C. Mohrig
ExxonMobil Upstream Research Company
P.O. Box 2189
Houston, Texas 77252-2189

Glenn T. Cayley
ExxonMobil International LTD.
Esso House, 96 Victoria Street
London, England SW1E 5JW

Abstract

A unique perspective of sand-rich, basin-floor fan deposition was gained through an integrated study of the Paleogene deepwater reservoirs in the UK Central North Sea. The data set included contiguous 3D seismic (8400 km^2), 2D seismic (11,100 km), well logs (350 wells), high-resolution palynology (180 wells), and core (30 wells). The study provided new insight into downfan changes in reservoir facies and architecture and a framework to understand fan evolution through both low- and high-frequency depositional cycles.

The Paleogene in this part of the basin is subdivided into four low-frequency (1-3 MY) composite sequences. Major basin floor fan cycles include the Maureen Formation, the Andrew-Lista units, the Forties-Sele-Balder units, and the Tay-Chestnut units. These low-order successions exhibit large-scale compensational stacking behavior and, in contrast to classical fan models, maintain channel-form patterns to their distal pinchouts. Sheet geometries are surprisingly rare. Sandstone body geometries, coupled with core-based lithofacies suggest that both turbidity currents and semi-cohesive sandy debris flows were active during reservoir deposition.

Each of the major sand-rich fan units (*e.g.*, Forties, Tay) is composed of higher frequency depositional sequences that display important changes in lithofacies and architecture through time. The early sequences are heterolithic consisting of variable proportions of mud-rich debrites and sandstones that are commonly thin and arranged into broadly channelized bodies (high aspect ratios). The later sequences are much sandier. The sandstone bodies show slightly sinuous to linear channel-form patterns (lower aspect ratios). Although less laterally extensive, the youngest sequences have high quality reservoirs that locally have strongly mounded cross-sectional geometries.

The vertical change in reservoir character reflects a progressive change in the composition and relative volume of the sediment gravity flows being triggered at the shelf edge and then delivered into the basin. Following initial phases of muddy debris flows and sandy turbidity currents, sediment gravity flows became progressively sandier and confined in discrete channels. Latest-stage sequences are locally dominated by sandy debrites. This pattern records the evolution of the lowstand shelf-margin system as it became progressively sandier and increasingly prone to large, sand-rich failures that maintained a semi-cohesive rheology as they flowed onto the basin floor. Superimposed on this changing sediment composition is a progressive decrease in sediment volume as more sediment is trapped on the shelf in response to the low-order rise in sea level.

This integrated seismic, lithofacies, and stratigraphic analysis leads to an improved regional (play) to local (field-scale) stratigraphic correlation and reservoir mapping methodology. This analysis also addresses variations in reservoir quality, channel geometry, and lateral and down-fan facies changes.

Introduction

This paper illustrates the application of high-resolution sequence stratigraphy to understand better and predict reservoir characteristics of basin-floor fans. This work stems from a regional-to-prospect-scale investigation of the oil and gas producing Paleogene deepwater sandstones of the Central North Sea where Esso UK and Shell UK have a high concentration of leases. The study integrates over 8400 km^2 of 3D seismic, over 11,000 km of 2D seismic and incorporated 350 well logs, and 180 wells having high-resolution palynology (Fig. 1)

Figure 2 shows the stratigraphic position of the major basin-floor fan cycles in UK central North Sea. The main fan-building phases are the Andrew/Lista, the Forties/Sele and the Tay systems. Most of the fan sediments in the central graben area belong to the Forties and Tay units. Previous studies by Neal (1996) and Den Hartog Jager *et al.* (1993) recognize the composite nature of these basin-floor fans. Their work demonstrate that the major fan cycles are not the response of a single, long-term sea level cycle but rather the result of a succession of higher frequency sea level cycles (Fig. 2).

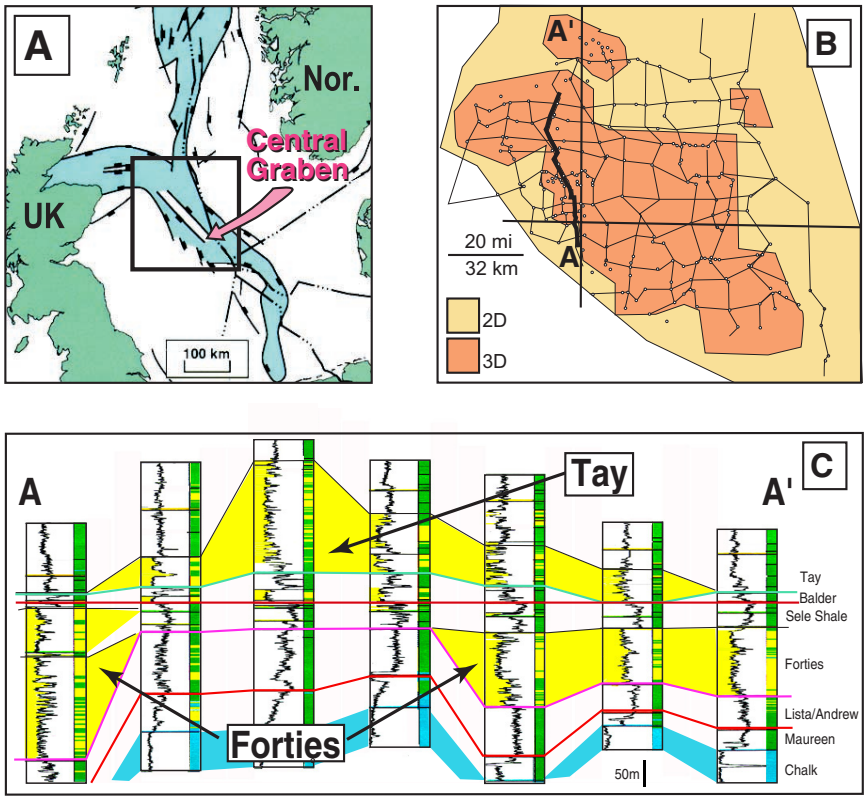

Figure 1. (A) North Sea regional map highlighting the configuration of the graben depocenters. This study focuses on the Central Graben. (square). (B) Focus area showing well log and cross section base and seismic coverage. (C) Regional well-log cross section showing the compensational stacking relationship between the Forties and Tay basin floor systems. Location of cross-section shown in Figures 1B and 3.

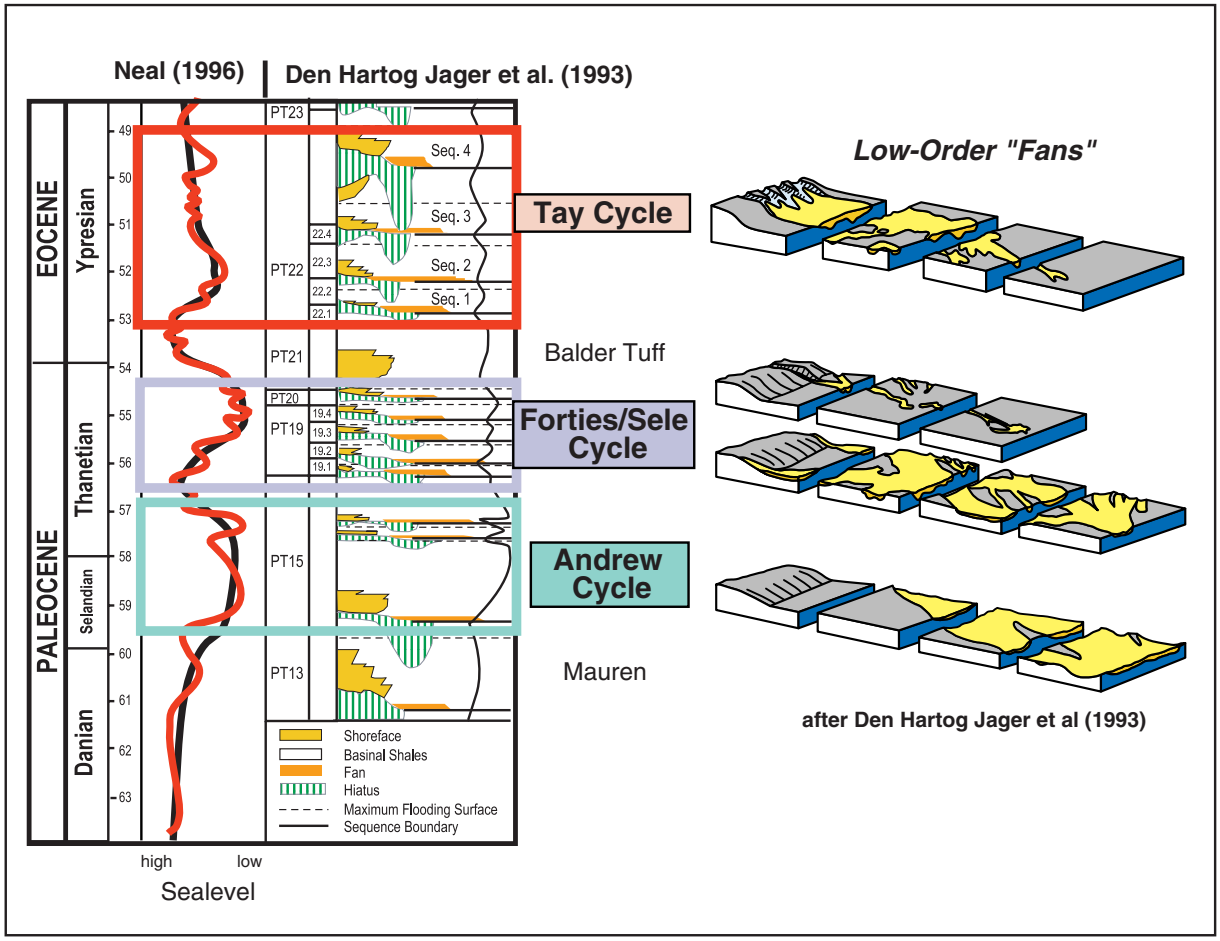

Figure 2. Chronostratigraphic chart for the North Sea that combines the work of Neal (1996) and Den Hartog Jager *et al.* (1993). Three major sea-level cycles have created the Andrew, Forties/Sele, and Tay composite fans. Both workers recognized that the composite fans were constructed of units that reflect higher frequency relative sea level variations that have biostratigraphic significance. The Forties fan is subdivided into four biostratigraphically distinct zones (19.1-19.4) and the Tay includes 21.1-23.5 biozones. Low order transgressive events separate the major fan building phases.

This paper examines on the high frequency sequence stratigraphy of the lower Eocene Tay and upper Paleocene Forties/Sele fans. Through this analysis, the temporal evolution of major fan systems are reconstructed and the controls on progressive changes in fan character are interpreted. We show that the high frequency sequences display systematic changes in sand percent, reservoir quality, architecture, and seismic geometries. We interpret these changes to reflect an evolution in the shelf-edge sediment delivery system which is controlled by shelf accommodation and sediment storage. We propose that low-order relative sea level helped drive the accommodation in this sediment source area. We begin with a discussion on large-scale fan distribution and follow with an examination of the upper of the two fan cycles, the Eocene Tay. A portion of the Forties/Sele cycle is then examined to show relevant aspects that are common between the two systems.

Sediment Delivery System and Large-Scale Fan Stacking Patterns

Paleogeographic reconstructions and basin-scale isochrons highlight basin-floor fan distribution of the Forties/Sele and Tay systems (Figs. 1 and 3). A major, first-order control on fan distribution is large-scale compensational stacking. The Tay fan is laterally offset from the Forties fan thicks even though both systems have been fed from the Outer Moray Firth sediment conduit. The bulk of the sediments came through this feeder system from the tectonically active Scottish Highlands that were uplifting due to underplating and volcanism toward the west.

The rate of terrestrial erosion was high. As much as 1 km/million years was being stripped off and redistributed largely as basin floor sediments (Den Hartog Jager *et al.*, 1993). A minor conduit also fed terrigenous sediments

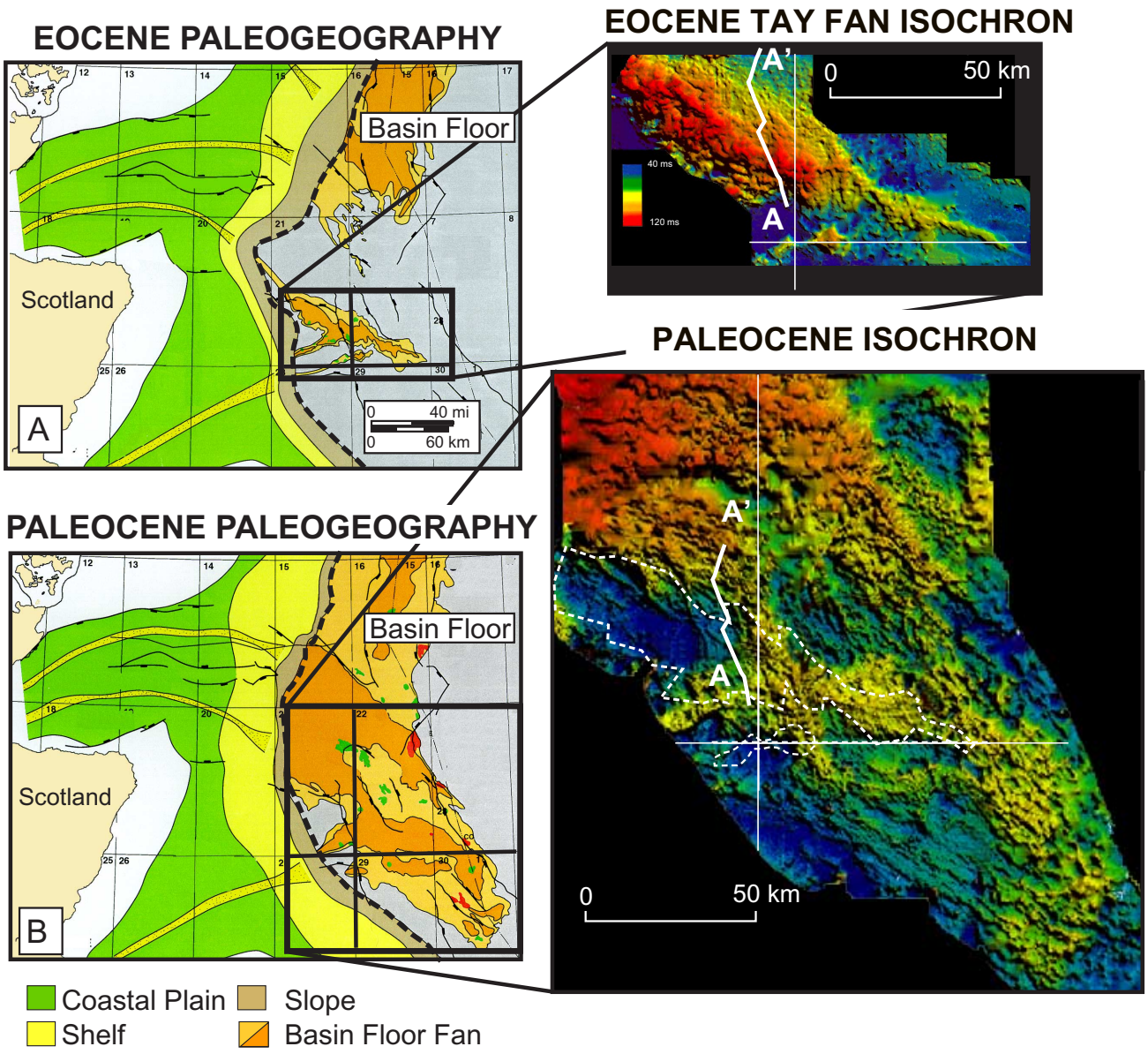

Figure 3. Regional paleogeographic expression of the Paleocene (largely Forties) and early Eocene (Tay) shelf-slope-basin floor systems. Paleogeographic reconstructions are based on well-log data and seismic facies. The Paleocene system includes all strata from the top Cretaceous Chalk to the base of the Balder Tuff, a regional tuffaceous claystone marker. In this part of the North Sea basin, the Paleocene isochron is dominated by sandstones of the Forties fan. Note the conduits that fed sediment to the basin floor. These interact to produce an apparent crossing pattern of basin floor sandstone-rich thicks during Paleocene deposition. The compensationally driven outline of the Tay fan is superimposed on the Paleocene isochron.

from the southwest. This conduit was active during the deposition of both fan systems.

Tay Fan Cycle

Nearly contiguous 3D seismic surveys calibrated to over 100 well-log synthetics enables an accurate characterization of the Tay basin-floor fan. The Tay rests on a well defined basin-wide marker called the Balder Tuff and is overlain by a thick succession of relatively monotonous shale. Therefore, the base and top of the fan cycle have strong acoustic impedance and are readily mappable. The Tay composite fan is a large, lobate, and distally tapering body nearly 125 km long and 40 km wide (Fig. 4). Well-log lithofacies, sand percent, and isochron have been integrated to create a composite facies distribution map (Fig. 4). Four relatively distinct units make up the Tay fan and are informally designated as Tay Sequences 1, 2, 3 and

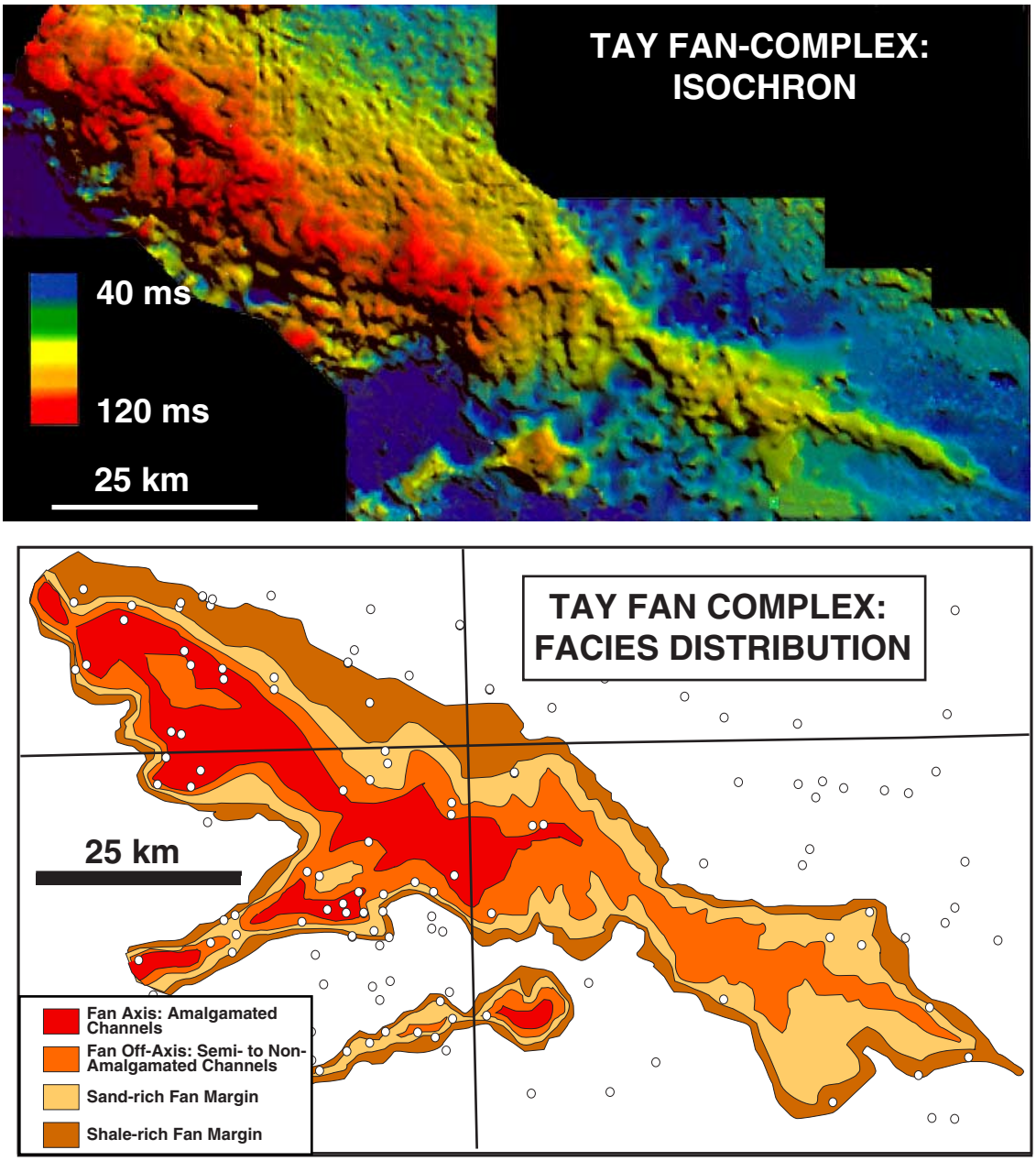

Figure 4. Detailed expression of the complete Tay Fan isochron and facies distribution map. Channels are the fan building blocks and sandstone-rich facies are identified based on the degree of vertical channel amalgamation. Local channels and a mixture of thin-bedded turbidites and debrites dominate fan-margin facies.

4 (Fig. 5) using 3D seismic and high-resolution palynostratigraphy. The maps show that the older Tay Sequences 1 and 2 have a greater basinward extent. The younger Tay sequences 3 and 4 are significantly smaller and stack in a back-stepping or retrograding pattern, giving important clues regarding the evolution in sediment volume available during the low-order lowstand sea level cycle.

Significant variations in sand percent and reservoir architecture exist between the sequences. From early to late, sand percent increases although the volume of sediment (fan size, extent) is decreasing. Figures 6 to 9 illustrate some of the seismic, core, and log expressions of these changes. Figure 6 is from the middle of the Tay fan and highlights characteristics of the lower two sequences. The well-log profiles consist of two distinct log facies. Sequence 1 is dominated by thinner bedded, lower sand percent facies and exhibits little facies change as it thickens to the right or into the axis of the fan. Sequence 2 is blockier, sand rich, and displays more obvious channel

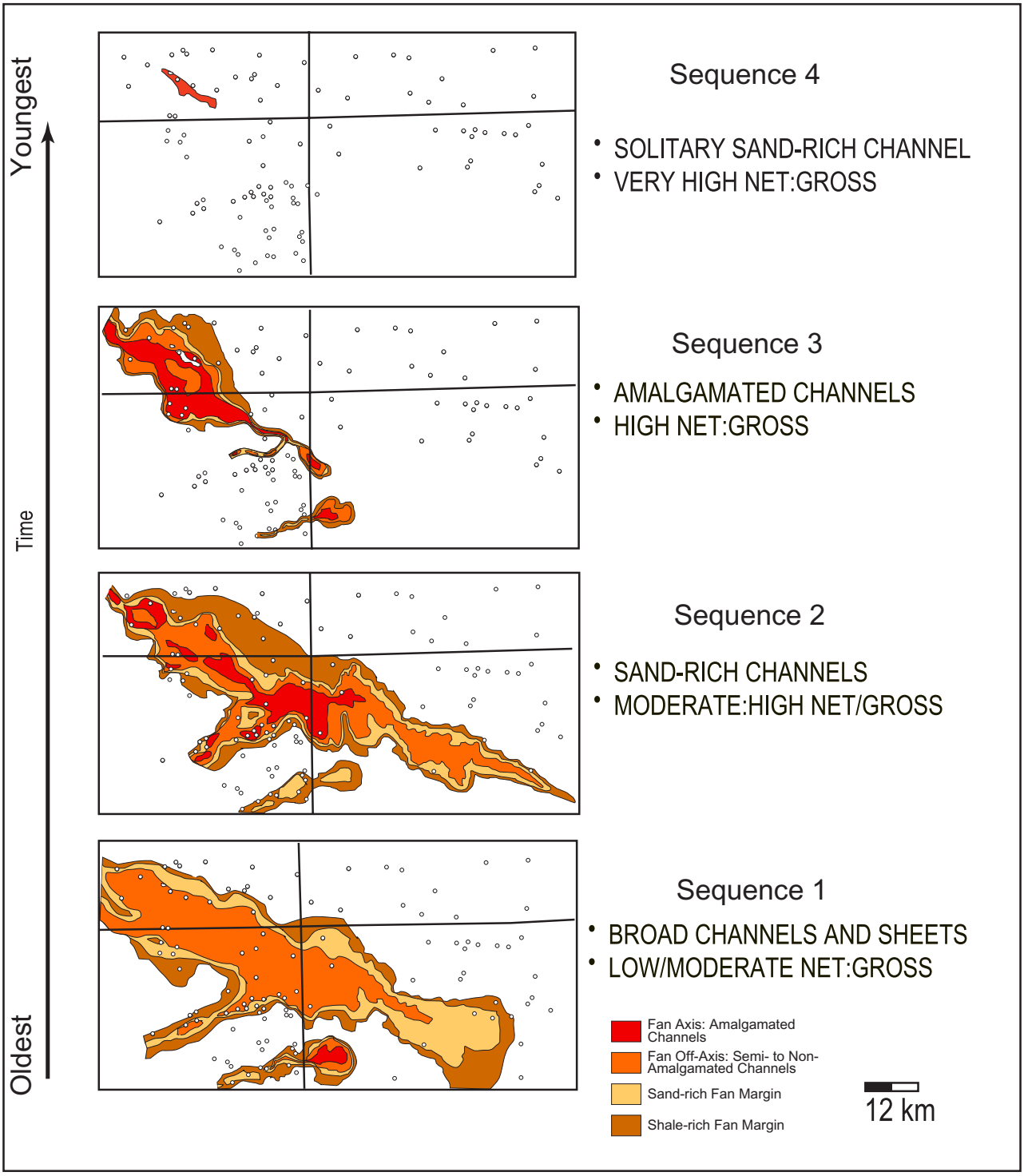

Figure 5. Individual high frequency sequence maps that together comprise the Tay composite fan cycle. Tay sequence 1 has a broad extent but has low to moderate sand percent and channels are thin to poorly developed. Sequence 2 is considerably sandier and has a higher proportion of fully amalgamated stacked channels. This sequence has the farthest basinward extent. Sequence 3 is much more restricted in extent and dominates the upslope portion of the fan area. Significant amalgamated thicks (>50 m) occur in this area. Sequence 4 is an areally small but thick (80 m), linear sandstone body having very high sand percent (>95%).

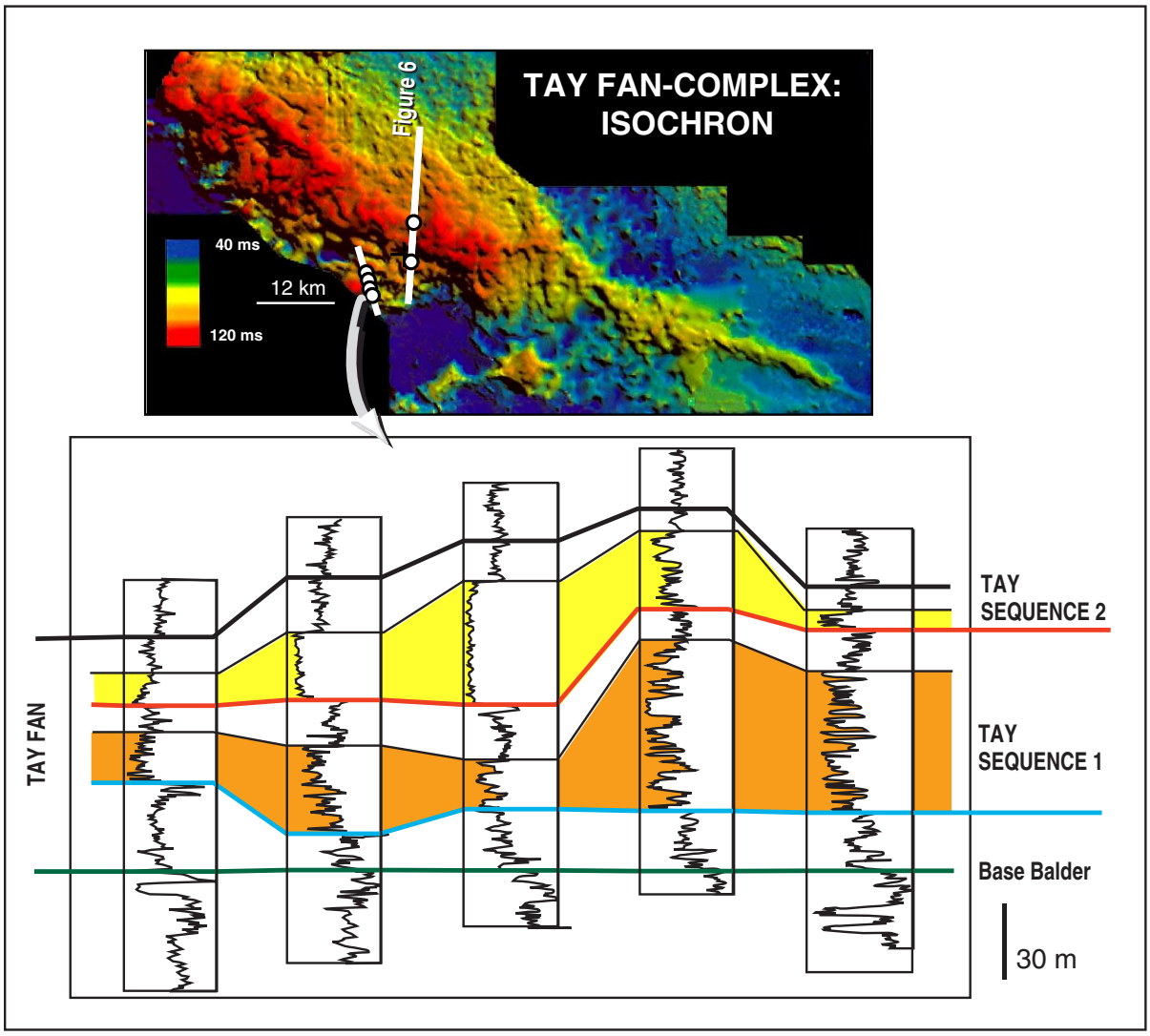

Figure 6. Tay fan isochron and well-log cross section of closely spaced wells showing the lithofacies contrast between Tay sequence 1 and Tay sequence 2. Sequence 1 is lower sand percent, thinner bedded and shows little sand percent variations into relative thicks. In contrast, Tay sequence 2 exhibits an amalgamated succession in the channel complex thick with high sand percent; marginal penetrations show thinner beds and a lower sand percent.

axis (massive, amalgamated) to channel margin (heterolithic, interbedded) changes in facies and architecture.

Regional mapping show these well-log patterns to be relatively fan-wide in extent. Figure 7 shows the seismic character and well-log patterns for the same two sequences farther to the north in the fan axis. Similar to Figure 6, Tay sequence 1 has a uniformly serrated well-log pattern with a low-amplitude, semi to discontinuous seismic facies. In contrast, Tay sequence 2 is dominated by massive sandstone. It rests on an erosional base and, at the well penetration, has an acoustically transparent seismic expression indicating a massive lithology.

Differences between the two sequences are well expressed at the distal fan pinchout. Sequence 1 shows a thin, broad, lobate pattern whereas Tay sequence 2 maintains a strikingly linear channel-form pattern (Fig. 8). Well A has penetrated the margin of the Tay sequence 2 isochron thick. Both Tay sequence 1 and Tay sequence 2 are thinly bedded at this location, but core from Tay sequence 1 shows the interval is highly heterolithic and disorganized. Floating shale and siltstone lithoclasts, carbonaceous mudstones, chaotic swirled bedding, and dewatering structures are abundant. The interval has a complex juxtaposition of clast-rich conglomerates, muddy and sandy debrites, and sandy and muddy turbidites. The complexity of this “distal fan facies” contrasts many classical fan systems which tend to be dominated by laterally continuous, thin-bedded turbidites. The isochron thick pattern and nearby well control show the Tay sequence 2 to be dominated by clean, turbidite sandstones containing a high

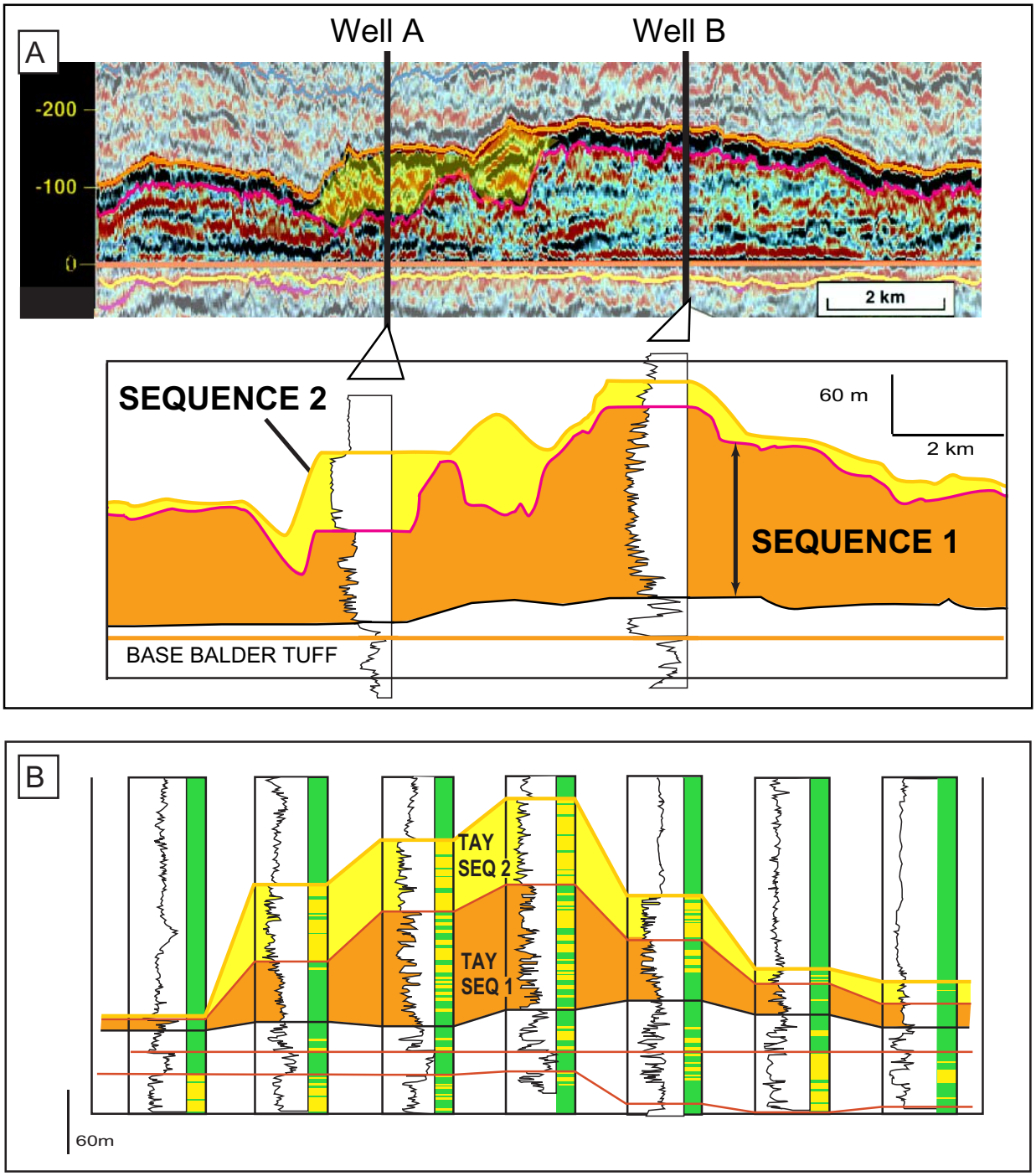

Figure 7. (A) Seismic/well-log profiles from the axial thick of the Tay fan. Note the much more heterolithic composition of Tay sequence 1 in contrast to the erosively based, massive sandstones penetrated in sequence 2 by well A. Wells are about 5 km apart. (B) Cross sections across the Tay fan. Note the lithofacies contrast between the two sequences.

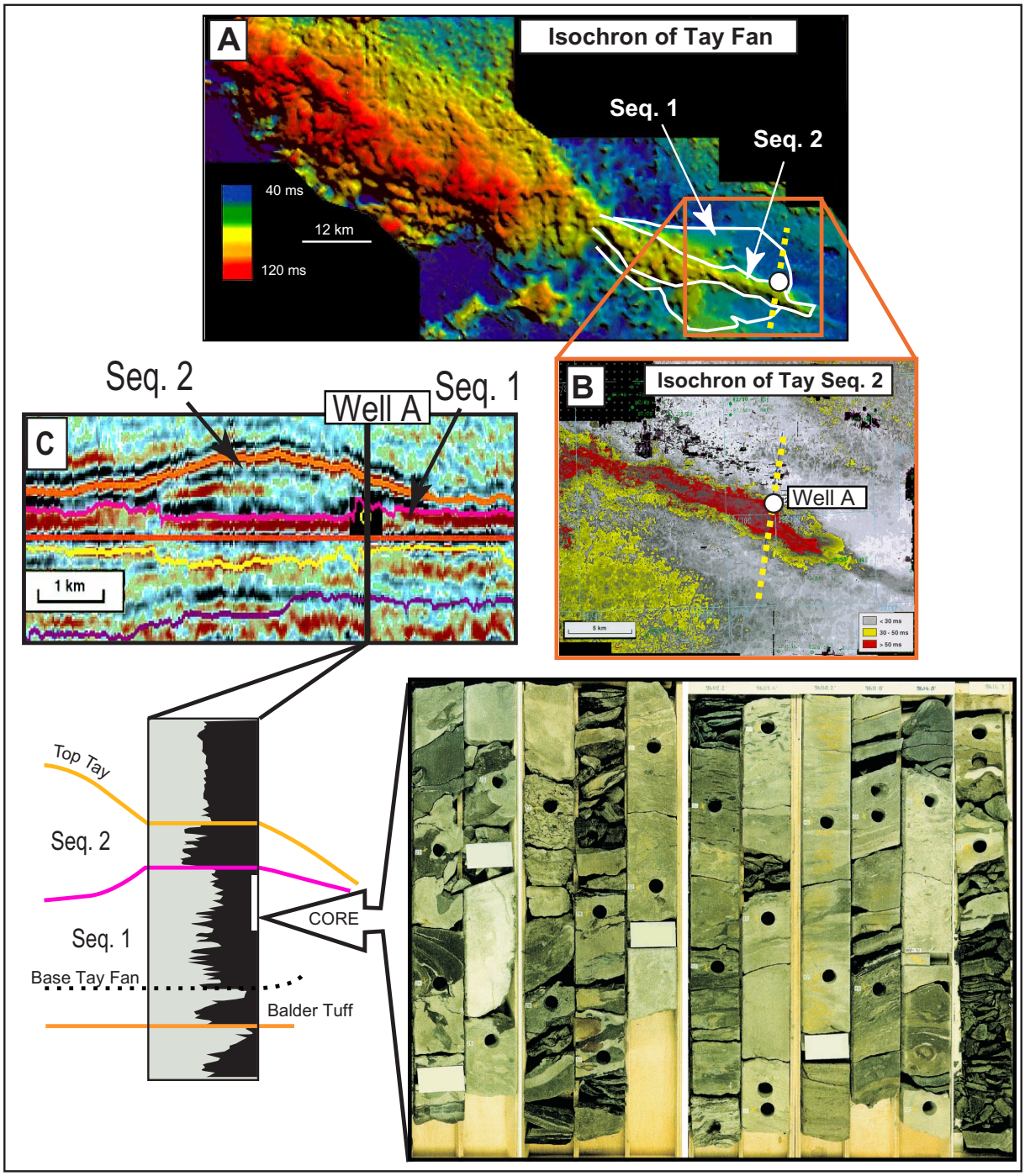

Figure 8. (A) Tay fan isochron showing the seismically defined limits of distal extents of sequence 1 and 2. Sequence 1 has a more paddle-shaped and uniformly thin pattern. Sequence 2 has a strongly linear, more channel form pattern. Note position of well A and the seismic profile (dashed line). (B) Detail of the distal fan highlighting the linear isochron pattern of sequence 2. (C) Seismic profile datumed on the base Balder tuff. The isochron thick is made up of almost entirely Sequence 2. Note well log pattern from Well A. Sequence 2 has a much higher sand percent than sequence 1. Nearby well penetrations in slightly more proximal positions show a very high sand percent, amalgamated sandstone succession in the axis of this sequence 2 thick. (D) Core from sequence 1. The interval is dominated by thin bedded, shaley sandstone displaying contorted and swirled fabrics and abundant angular shale lithoclasts that are poorly organized. Porosity and permeability is low. The interval is interpreted as a succession of cohesive mud-rich sandy debrites with minor thin-bedded turbidites.

sand percent. Muddy/sandy debrites seen in Tay sequence 1 are absent in sequence 2 in this locality and throughout the fan. Also note that sequence 2 has a strongly linear, distally tapering channel form having no apparent lobe-like terminus. These relationships further contrast turbidite-dominated, classical-fan systems.

Tay sequences 3 and 4 display relevant changes in sand percent and geometry. Tay sequence 3 has a much more restricted distribution than sequences 1 and 2 as the bulk of this sequence is deposited in the upper reaches of the fan closer to the coeval toe of slope (Fig. 5). Sequence 3 is characterized by thin to very thick intervals (>120 m) of sandstone and minor shales (*e.g.*, Well A, Fig. 9C). No core was recovered from this part of the succession so little is known of the lithofacies composition of this sequence.

A unique channel-form body makes up Tay sequence 4 (Figs. 5 and 9). This biostratigraphically distinct unit forms a very localized sandstone body, which sits in strong positive relief on the older Tay fan sequences (Fig. 9D). The isochron shows abrupt upslope and downslope terminations. Well B has penetrated over 140 m (450 ft) of sandstone. The unit shows a strongly mounded geometry having a gently concave-up basal surface. The degree of mounding is significant and the geometry of this sandstone body has been reconstructed or decompacted to determine what was the pre-burial geometry when it came to rest on the sea floor (see below). Downslope and to the southeast, the channel form body divides into two discrete, abruptly terminating finger-like lobes. These lobes have very blunt noses and slope angles of 10 degrees. Note that in the well tie line (Fig. 9D), little to no sequence 4 sand is found outside of the well-defined isochron thick.

Forties/Sele Composite Fan Cycle

Similar to the Tay composite fan, the Forties fan is composed of several biostratigraphically distinct units that are interpreted as high-frequency sequences (Neal, 1996; Den Hartog Jager *et al.*, 1993). The long-term fan cycle applied in this study includes the four biozones that make up the Forties and the biozone that occurs in the dominantly hemipelagic shale of the Sele (Fig. 2). We know less about the fan-wide high frequency stratigraphy of the Forties/Sele fan in comparison to the Tay cycle because high-resolution biostratigraphy and detailed seismic mapping of Forties/Sele cycle is restricted to areas around undrilled prospects and within highly drilled oil and gas fields.

Some of the trends encountered in the Forties fan are observed from a highly drilled field in the UK central graben. A field-scale example is shown in Figures 10 and 11. The Paleocene Forties is subdivided into four distinct and mappable sequences in this field. Vertical changes in sandstone body architecture and sand percent are observed. The discontinuous mounded patterns from Forties sequence 1 are calibrated using core to a heterolithic association of sandy and muddy debrites and sandy channelized turbidites. Isochron patterns are discontinuous and segmented, and locally highly mounded. sequence 2 is the thickest sequence and composed of well-defined, erosive channels to highly vertical and lateral amalgamated channels to form sandstone-rich channel complexes. Sequences 3 and 4 remain channelized but have appreciably lower degrees of amalgamation suggesting a lower sand influx. However, all of these sequences are very sandstone rich. Figure 11 shows a series of best-fit lines through all of the well data and relates sand percent to interval thickness. A systematic evolutionary trend of increasing sand percent occurs upward in the sequence set. For example, for a 30 m interval thickness, average sand percent is 40% for sequence 1, 50% for sequence 2, 64% for sequence 3, and 78% for sequence 4. The average sand percent nearly doubles for this interval thickness from Sequences 1 to 4. This example highlights why sequence stratigraphy should be used to more accurately map sandstone distribution away from well control.

Sandstone bodies of similar geometries and lithologies to the previously describe Tay fan cycle, cap the Forties/Sele fan cycle. Although the Sele is mainly a draping hemipelagic shale unit, sandstone bodies are encountered and many display linear and highly mounded geometries (Figs. 12 and 13). This feature is 1 km wide and occurs about 30 km from the toe of the coeval slope. The transverse profile shows narrow, mounded, and weakly to non-erosional geometry. The three-well cross section shows that well B penetrates 75 m of Sele sandstone, whereas wells A and C have encountered no Sele-age sandstone. The down-axis profile extends down-slope from Well B to the nearest penetration, well D. This profile shows a systematic thinning toward the basin as an abrupt, finger-like pinchout. Well D has no Sele. The core from the Sele sandstone in Well B consists of well sorted, high-quality massive sandstone, dewatering structures, and local outsized floating clasts (Fig. 14). The sandstones in the Sele are enriched in detritial glauconite. Classical Bouma sequences indicative of turbidity-current deposits are notably absent.

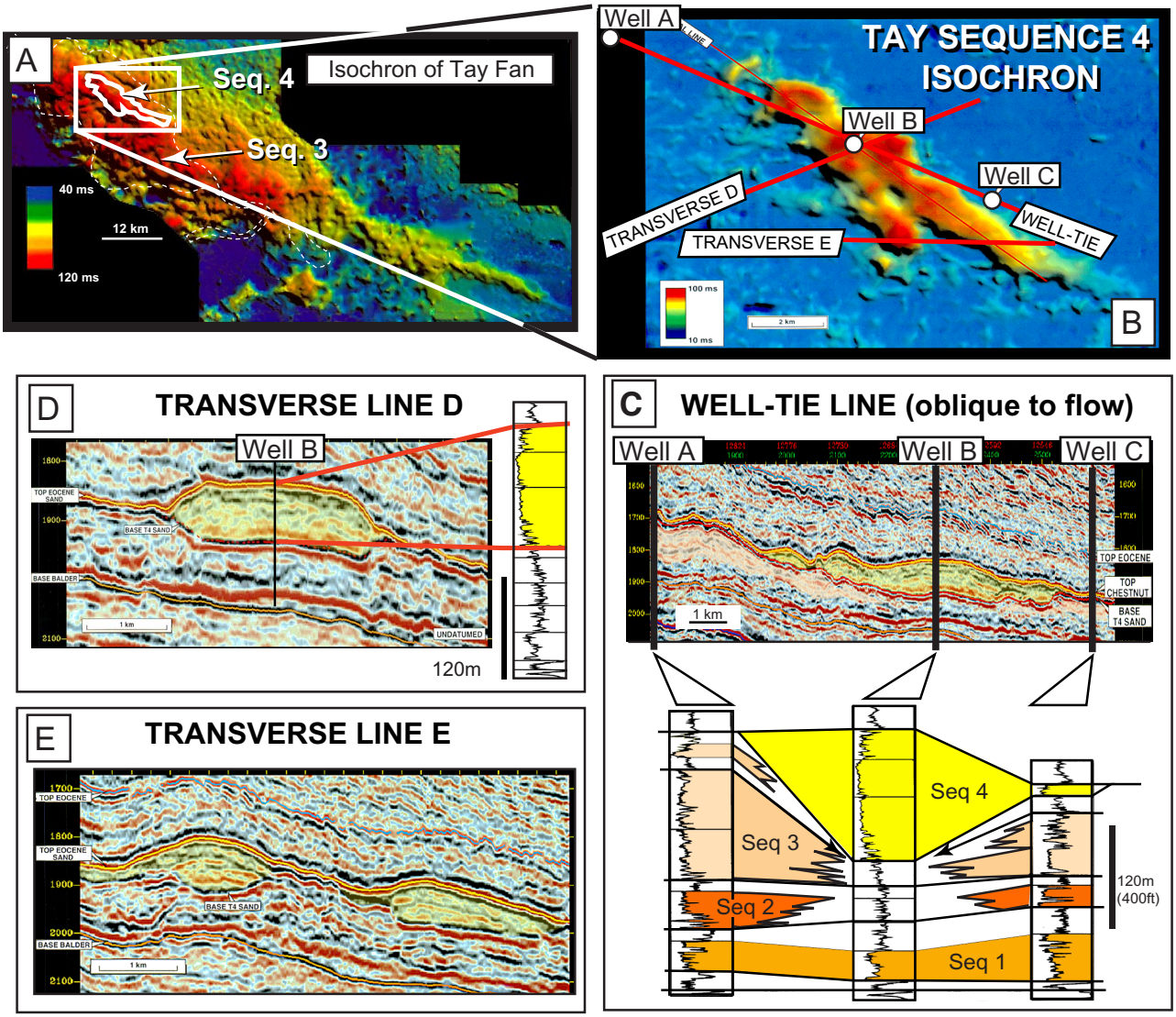

Figure 9. (A) Isochron of the Tay fan superimposing with the outline of the Tay sequence 4. This position is near the toe of the pre-existing slope. (B) Detailed isochron of Tay sequence 4 showing abrupt upslope and downslope terminations. The sandstone body is about 9 km long and 2 km wide. Note the downslope bifurcation into two finger-like lobes. (C) Well tie line, oriented obliquely across sandstone body. This line crosses well penetrations A, B, and C. Well-log correlations are based on palynology and seismic. Note that no sequence 4 sandstone is present in well A and only a thin blocky sandstone interval is found in Well C which penetrated the margin of the feature. No seismically resolvable sequence 4 sandstone is found downslope of this sandstone body. (D) Transverse seismic line across Well B. Note the strongly mounded seismic geometry and relatively weak erosional confinement. The sloping margins of the sandstone body decompact to range between 5 and 13 degrees. Well B encountered 130 m of very high interval-percentage of sand. (E) Transverse seismic profile B, slightly downslope from D. The strongly mounded profile with weak basal erosion is maintained.

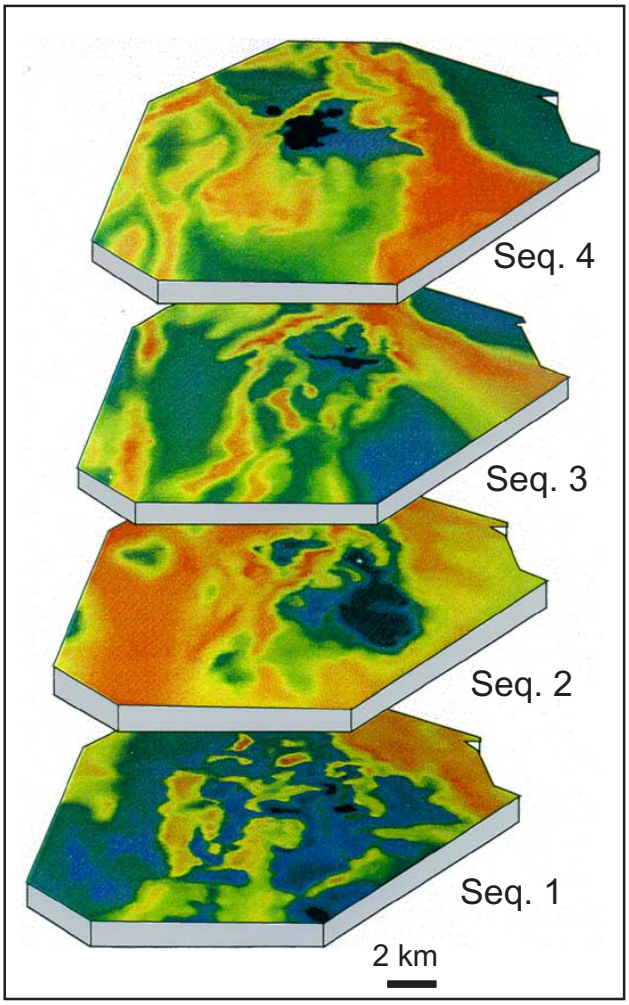

Figure 10. Isochron patterns of high frequency sequences mapped from a highly drilled field from the Forties fan. Similar to the Tay fan, the Forties is divisible into several sequences that show differences in sandstone body geometries and sand percent. Sequence 1 is composed of highly segmented to mounded bodies. Sequence 2 is thick, sandstone rich and composed of highly amalgamated channels. Sequences 3 and 4 are thinner at this locality but consist of amalgamated channel sandstones inside isochron thicks.

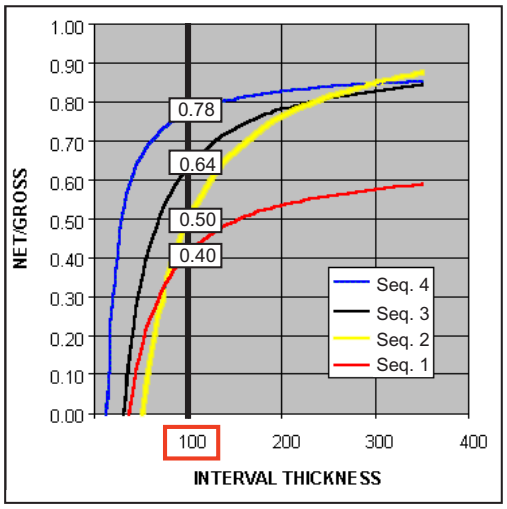

Figure 11. Plot of well log sand percent versus interval thickness by sequence for the field shown in Figure 9. The Forties fan shows a systematic increase in sand percent through time. For a given interval thickness such as 100 ft (30 m), sand percent for sequences 1, 2, 3, and 4 are 0.40, 0.50, 0.64, 0.78.

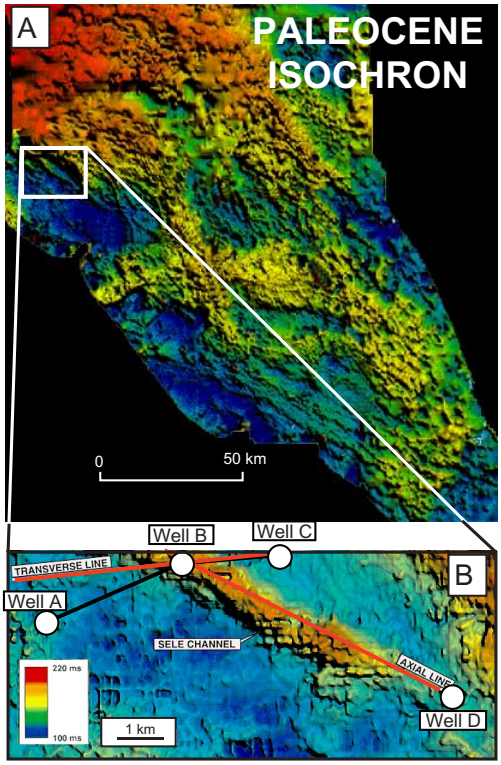

Figure 12. (A) Regional Paleocene isochron. Thicks approximate the sandstone distribution for the Forties fan and locally the Sele sandstones. The box highlights the position of narrow Sele-age sandstone body. This position is approximately 30 km from the coeval toe of slope. (B) Isochron of the Sele sandstone body. The unit extends upslope north of the 3D survey but clearly terminates in the basinward direction near the position of Well D. Transverse line and the axial line are shown in Figure 13.

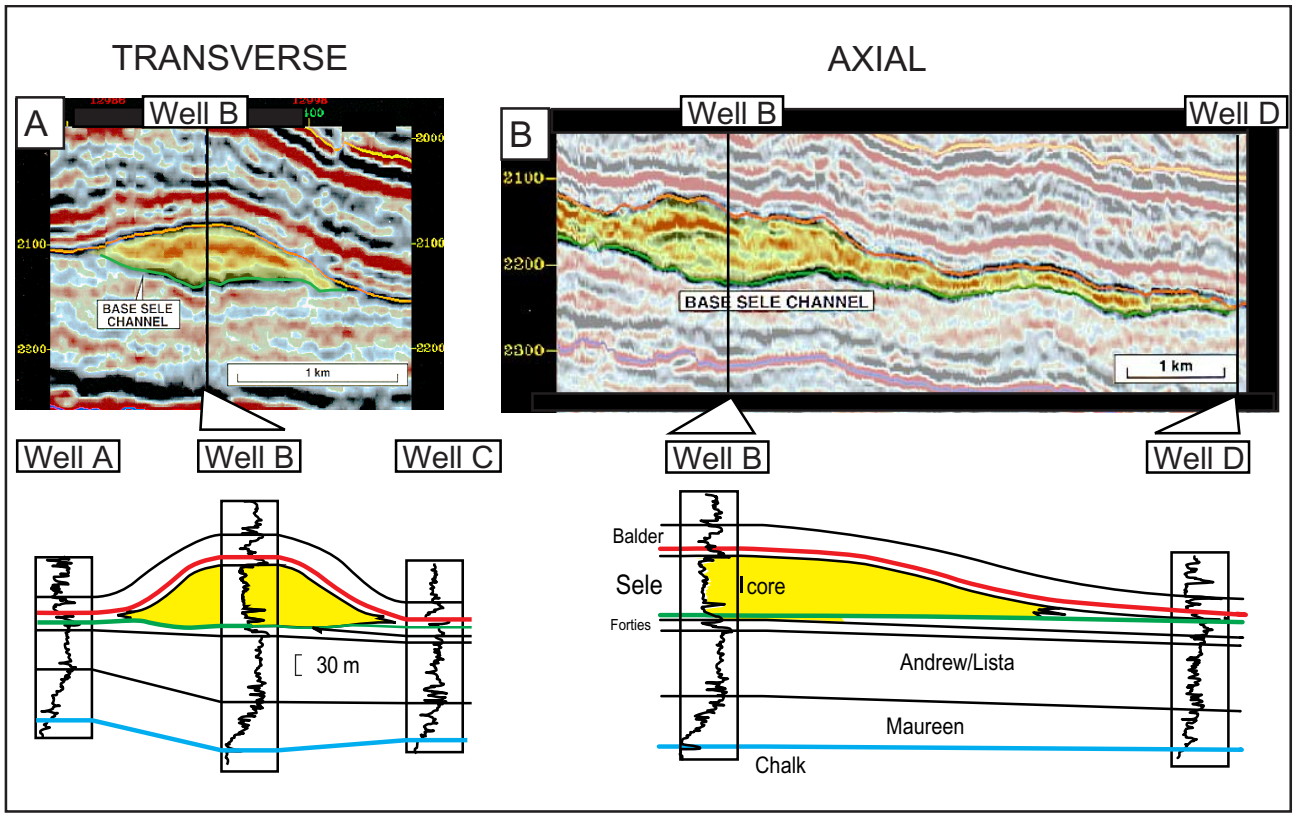

Figure 13. (A) Transverse seismic profile and well-log cross section. Well B has penetrated nearly 75 m (250 ft) of amalgamated, massive sandstone. Similar to the Tay sequence 4 sandstone body, this Sele sandstone example is mounded but has little to no confinement. No Sele sandstone is encountered in wells A and C. (B) Axial seismic and well-log cross-section. The seismic shows a downslope tapering of the sandstone body and has pinched out by Well D.

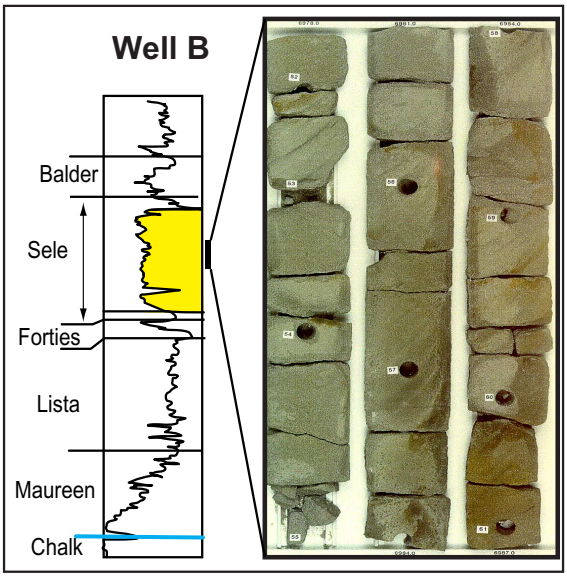

Figure 14. Core and log from the Sele sandstone in Well B. The interval is dominated by fine- to medium-grained, massive bedded sandstone displaying locally abundant pipe and dish structures. The well-sorted sandstone also is relatively rich in detritial glauconite implying a shallow marine shelf source.

Interpretation

Evolutionary Trends and Depositional Model

The higher frequency building blocks observed in the Forties and Tay fans display important changes in lithofacies and architecture through time (Fig. 15). For discussion purposes, the long-term fan/sea level cycle is divided into an early falling limb and a late rising limb. Tay and Forties high frequency sequences 1 and 2 are interpreted to sit on the falling limb and Tay and Forties sequences 3 and 4 and the Sele Formation sit on the rising limb. Initial sequences contain an abundance of mud-rich debrites. Sand-rich units are commonly thin and arranged into broadly channelized bodies (high aspect ratios). This is followed by the main fan-building phase during the peak lowstand (sequence 2) when both high and low frequency sea level falls are in phase. The rising limb sequences are more problematic in the context of rising low order sea level. These basin floor deposits are sandier and have sandstone bodies that show slightly sinuous to linear channel-form patterns (much lower aspect ratios). Although less laterally extensive, this phase of fan building leads to

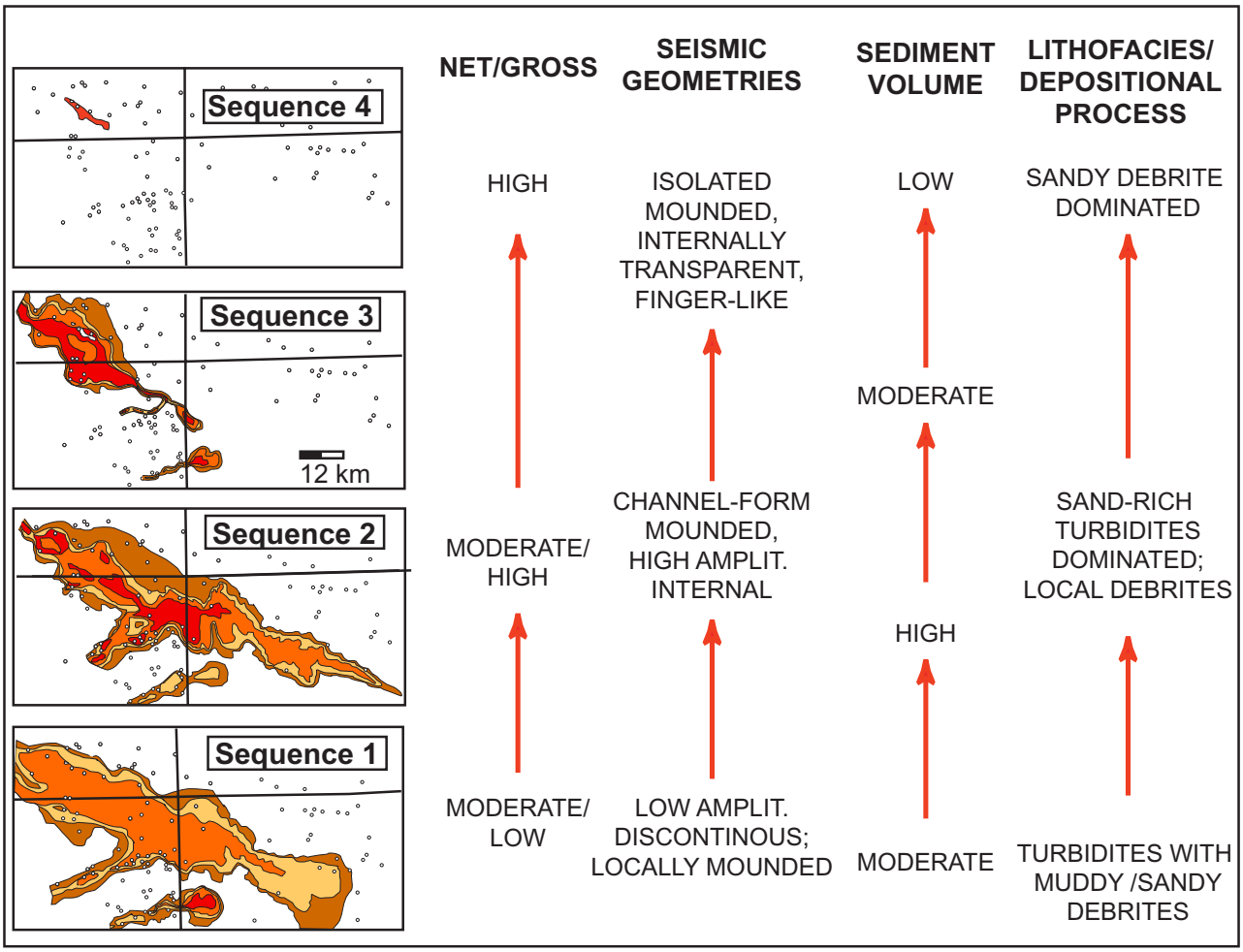

Figure 15. Stratigraphic Patterns and Interpretation. Sand percent patterns are observed from core and log. Seismic geometries are gained from the abundant 3D seismic coverage. Sediment volume is interpreted from the stacking patterns of facies, isochron, and isochore maps. Lithofacies and depositional process are interpretation from the integration of core and log data with seismic facies and map-view and cross-sectional geometries.

high quality reservoir sandstones that have strongly mounded cross-sectional geometries. Some of the sandstone bodies from the upper sequences are interpreted as sandy debrites. This is based on reconstructed depositional geometries using decompaction analysis and is presented below.

In this section a depositional model is proposed that attributes evolutionary patterns to reflect a coeval evolution of the lowstand shelf-margin system. This system becomes sandier and increasingly prone to large, sand-rich failures during the later-stage fan deposition. The low-order rising sea level drove both the progressive increase in the sand-rich shelf edge as well as a progressive decrease in sediment volume being delivered to the basin floor.

The interpreted evolution toward debris-flow (visco-plastic rheology) processes is based on the combination of decompaction analysis to reconstruct sea floor sand-body geometry at the time of deposition and lithofacies analysis from core (*cf.*, Shanmugam *et al.*, 1995). A quantitative representation of original sand body morphology is required before these geometries can be qualitatively attributed to specific flow processes. This has been achieved via reconstruction of the pre-burial geometries of the sandstone bodies using standard decompaction algorithms. A mounded geometry can be created in several ways. Mounding is generated when a simple sandy channel encased in more compactable muddy substrate is progressively buried (Fig. 16A). For example, the thinning of a 20 m thick column of shale associated with 500 m burial under conditions of normal fluid pressure leads to a 50% reduction in shale column thickness, whereas a similar column of sand is reduced by only 15%. This substantial difference in the compaction of substrate and channel-fill material creates compactional mounding. It is important to keep in mind that the production of mounding

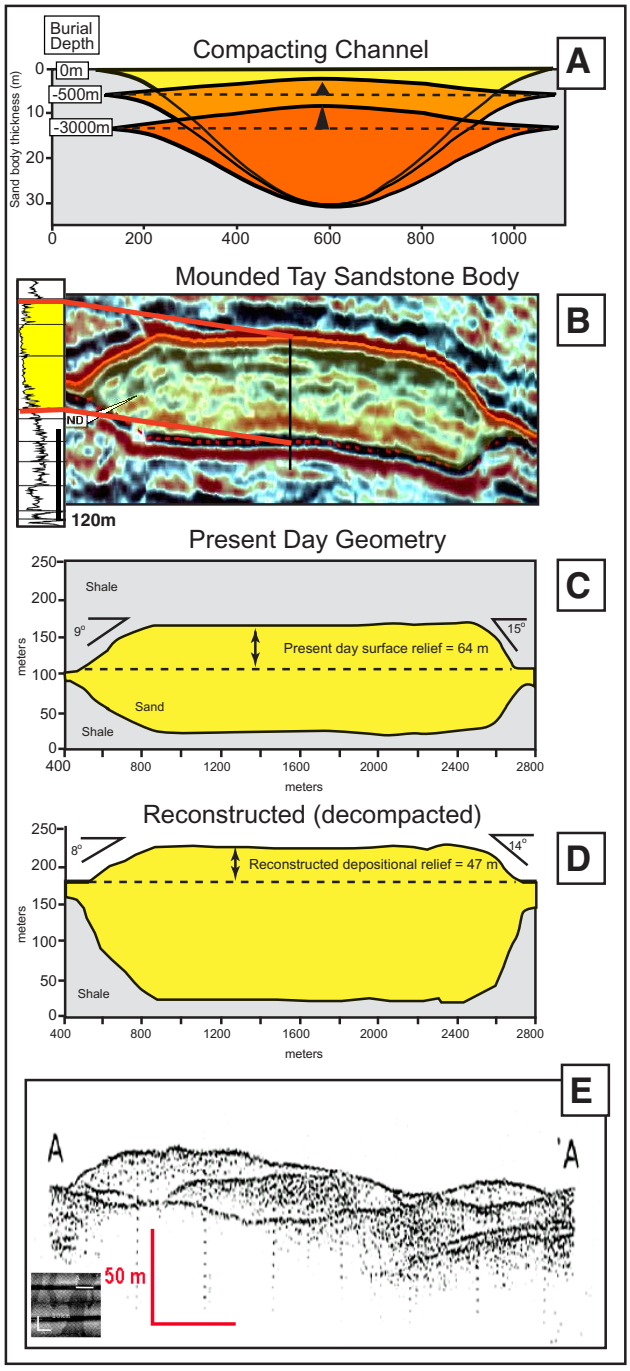

Figure 16. Compaction modeling of mounded geometries. (A) Example of channel-profile change and the development mounding due to differential compaction of channel sands and encasing muds. Three states of channel burial are shown: 0 m, 500 m, and 3000 m burial. The black triangles indicate the amount of relief above the container margins that is attributed to differential compaction. (B) Seismic profile of the Tay sequence 4 sandstone body. The feature is currently at nearly 2000 m below the sea floor. (C) Profile of Tay sandstone body after removal of structural deformation. Approximately 64 m of the 140 m thick sandstone sits above the container margins (dashed line). Note the high margin slope angles range between 9 and 15o. (D) Sandstone body reconstructed or decompacted to geometries probable at the paleo-seafloor. Forty-seven meters of sand remains above the container margin and slopes remain high, ranging between 8 and 14o. Classical turbidity flow processes do not generate this amount of excess sand above confining boundaries or these high slope angles. (E) Bear Island fan showing mounded geometries attributed to debris flow deposition (ElverhØi *et al.*, 1997). Note the surface slopes of these debrites steepen into their margins, giving them a convex-upward shape.

by differential compaction stops when the substrate (mud) and channel fill (sand) porosity vs. depth curves become sub-parallel. From this point forward, the substrate and the channel fill are thinning at approximately the same rate. The algorithms used predict that significant production of mounding by differential compaction will cease at a burial depth of about 300 m. The maximum amount of compactional mounding will develop where a channel complex entirely composed of sand sits in an erosional container entirely composed of clay. An example of the mounding that develops in this case is shown in Figure 16A. The change in cross sectional shape of channel fill is calculated using porosity versus depth curves for sand and stiff shale from Angevine *et al.* (1990). The ratio of the positive relief associated with mound generation (black triangle) to the basal relief associated with channel incision is always less than 40% for the first 3000 m of burial. The exact relationship between the positive and negative relief on a channel form will depend on the initial porosity values of the sand and the shale and on the depth of incision. Our analysis of the spectrum of possible cases leads us to conclude that mounding relief solely produced by differential compaction should never exceed the basal relief on a buried, confined-channel complex.

For the reconstruction of the Tay sequence 4 sandstone body (Fig. 16B) a relatively clay-rich shale decompaction curve has been selected because it yields the maximum estimate of the amount of mounding produced via differential compaction and a conservative estimate for the original depositional mounding. Both the present-day and decompacted shape of the sandstone body is shown in Figure 16 A and D, respectively. Presently, the mounded element has 64 m of positive relief and the decompacted body has 47 m of positive relief. This means that differential compaction of the sandy element and the shaly substrate accounts for no more than 30 % (17 m) of the surface relief. We therefore conclude that at least 70% of the observed mounding is depositional in origin. That is, the sand body had tens of meters of positive relief on the paleo-seafloor.

The observed magnitude and style of this relief is consistent with the deposits of submarine debris flows. These

flows are dense mixtures typically composed of 45-65% sediment and 35-55% water by volume. These sediment concentrations are substantially higher than those found in turbidity currents. Sediment concentrations are high enough in debris flows to hinder the motion of fluid around the grains. Debris flows, and particularly sandy debris flows, owe their mobility to the fact that velocities at which water passes through the assemblages of grains are typically at least 1000 to 10,000 times lower than the velocities at which the flows travel down slope. The sediment and water therefore "effectively" combine to move down slope as a single phase and these flows are very rarely turbulent.

Recent experimental and theoretical studies on concentrated mixtures of sediment and water have built a framework for understanding the transport mechanisms and depositional processes associated with sandy debris flows, *i.e.*, sediment mixtures with less than 5% mud. (Iverson, 1997; Shanmugam, 1996; 2000). This body of work clearly demonstrates that debris flows can move very long distances on low slopes even when these mixtures are lacking a significant clay fraction to bind with the water, thereby increasing the viscosity and the density of the pore fluid. For many distributions of grains, water alone filling pore spaces can reduce the grain friction to the point where the mixture can flow. Water reduces the internal friction by maintaining pore pressures that are high enough to liquefy these sandy flows. These nearly lithostatic pore pressures typically develop at the time of failure, during flow mobilization and acceleration. The pore water can continue to lubricate the flow until the expulsion of pore water produces a decreased pore-fluid pressure and increased intergranular friction that can cause particle interactions to "grind" the flow to a halt. The time scale for the dissipation of these excess pore pressures can be long relative to the travel time of a sandy debris flow. In these cases, high pore pressures can be maintained throughout flow deceleration and deposition. Large-scale debris-flow experiments by Major and Iverson (1999) shows that pore pressures balancing the weight of the sandy debris (4% mud) persisted in the debrite for more than an hour after its deposition. Water-escape structures observed in the deposits of sandy debris flows indicate that the primary dissipation of lubricating, excess pore water occurs during post-depositional sediment consolidation.

We interpret that this Tay sand body is generated by a sandy debris flow having sufficient strength to develop steep depositional margins. The relief on the reconstructed geometries is compelling evidence for both the Tay and Sele example (Fig. 17). In addition, analyses of modern and ancient debrites show that surface slopes typically steepen into their margins, giving them a convex-upward shape (Figs. 16 D, E; 17) (*e.g.,* Elverhøi *et al.*, 1997). The steep marginal slopes are interpreted to be reflect debris

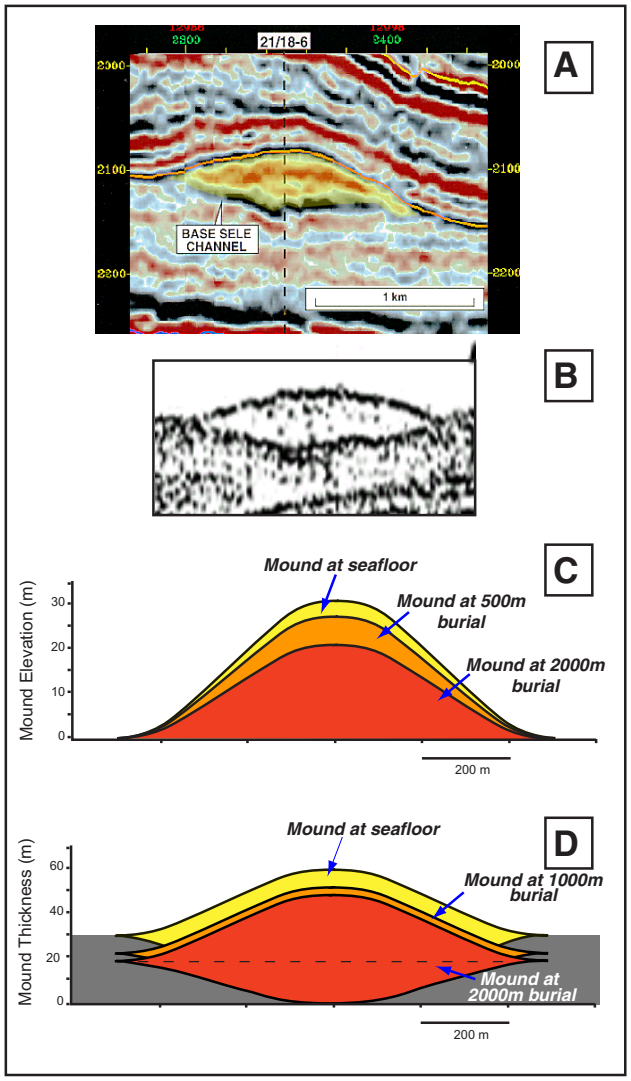

Figure 17. Two end-member cases depicting depositional mounding and the mechanical compaction more analogous to the Sele sandstone example. (A) Seismic profile of the Sele channel. (B) Zoom view of single debrite mound from Bear Island fan deposition (ElverhØi *et al.*, 1997). (C) The compaction evolution of an unconfined, strongly mounded element. In this case mechanical compaction only acts to thin the deposit, thereby decreasing the surface slopes associated with it. Since the deposit sits on top of a relatively flat surface, no compactional mounding will develop with burial so long as substrate is approximately homogeneous in composition. (D) Compaction of a confined, strongly mounded element. The primary mounding and the mechanical compaction combine to produce almost no change in the surface slopes and a small increase in the overall degree of mounding. Surface slopes remain approximately constant because the thinning of the sandy mound, which acts to reduces slopes as seen above, is counteracted by the relative subsidence of the margins of the element associated with the differential compaction of the element and its hosting substrate.

flows "freezing" in place as soon as the flow thins to the point where the gravitational driving stress drops below the yield strength of the debris slurry. These marginal slope geometries stand in stark contrast to the constructional flanks from modern levees. Levees commonly display concave-up profiles with maximum depositional slopes less than 4^{o} that systematically decrease with distance from the channel.

Changes in the Shelf-Edge Delivery System and Fan Evolution Patterns

Important clues are found at the coeval shelf-related sediment delivery system that may account for the observed changes in the basin-floor deposition. Although the 2D seismic and well data is sparse, we get a glimpse a possible mechanism that explains the sandier nature of flows late in the fan cycles. A seismic line from a coeval Forties/Sele cycle shelf shows a systematic increase in the dips of the shelf/slope clinoforms as the units were prograding into the basin (Fig. 18). Nearby wells show that this clinoform dip trend is coincident with progressively sandier, higher angle clinoforms.

The increase in clinoform dip is interpreted to reflect the delta's response to an increase in accommodation or the space available for sand to accumulate. Increasing accommodation promoted the trapping of coarse clastic sediment on the shelf/slope system and sediments were therefore less readily bypassed into the basin. As the shelf edge got sandier, the sediment gravity flows naturally became sandier too. We envision a system of oversteepening of sand-rich shelf margin deltas that catastrophically failed and sent well-winowed, glauconitic sand downslope via debris-flow processes. The lack of confining margins or levees in both the late-stage Tay and Sele systems further suggests that a relatively small percentage of muds accompanied the sediment gravity flow.

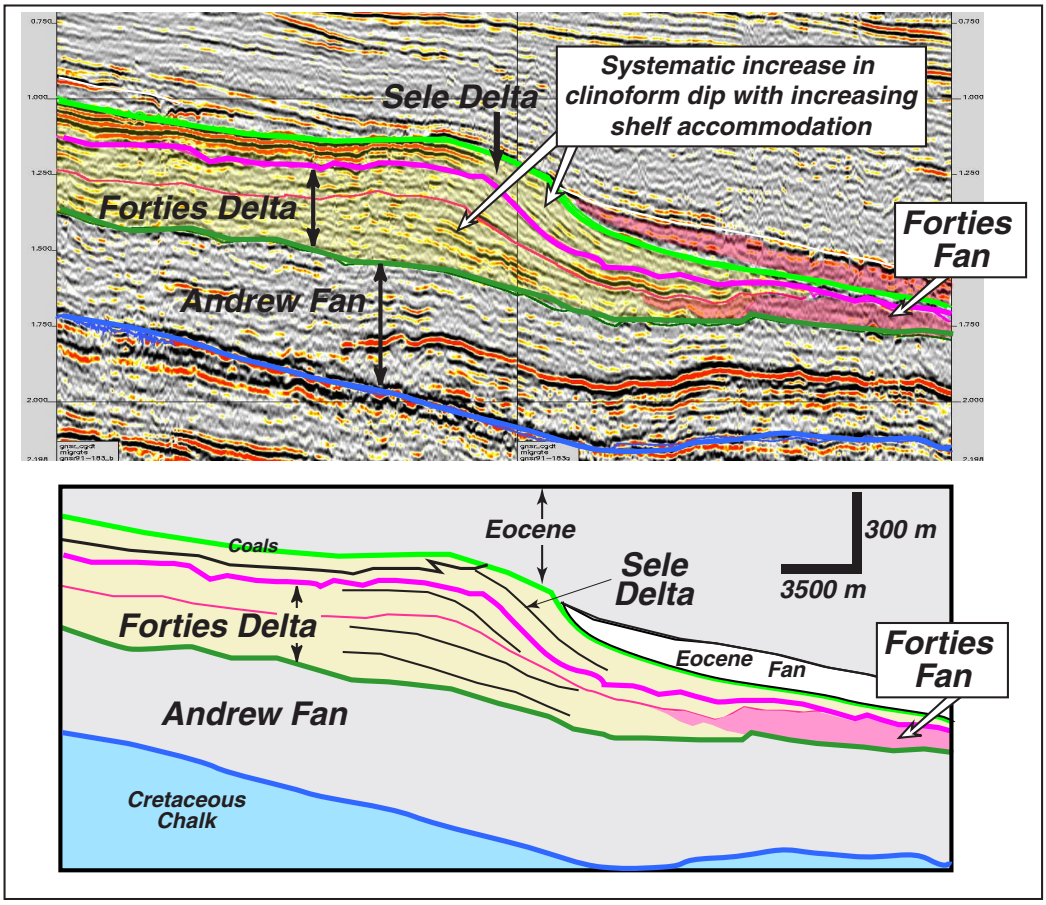

Figure 18. Sequence stratigraphic characteristics of the Forties/Sele delta complex. The systematic increase in clinoform dip is produced by the combination of high sediment supply and increasing low-order accommodation. Note the first significant coal accumulation on the delta topset occurs with the post-Forties Sele transgression. Although well data is sparse, increasing clinoform dip is coincident with increasing sand content. Consequently, sand supply was sufficient throughout the cycle to enable sand-rich delta progradation even though accommodation was increasing significantly around the basin.

The shelf-edge sediment delivery system likely underwent important evolutionary changes during the Paleogene fan cycles. These changes governed the caliber and supply of sediment to the basin floor. Figure 19 plots characteristics such as sand percent and flow character against interpreted low-order accommodation cycles. The high-frequency lowstands that ride on the low-order falling segment of the cycle have markedly different flow character than the sand-rich and debrite-influenced lowstands associated with those sequences riding on the rising phase of the cycle. Using a simplistic relative sea level sinusoid to modulate sediment supply, accommodation and eustatic forces, the falling limb sequences are heterolithic and high volume due to the prevailing shelf bypass and more continuous fluvial input of both sands and suspended muds. During the rising limb, more sand is trapped or stored on the shelf due to progressively increasing accommodation. Prior to failure and mass movement into the basin, sands on the shelf-edge are effectively winnowed of their fines. Consequently, relatively clean, well-sorted and potentially glauconitic sands undergo shelf-edge failure and mass wasting during high frequency lowstands. These catastrophic debris flows travel into the basin to create the highly mounded, abruptly terminating deposits. A compelling argument can be therefore made that the Tay sequence 4 sandstone body may represent only a few catastrophic shelf-edge failures.

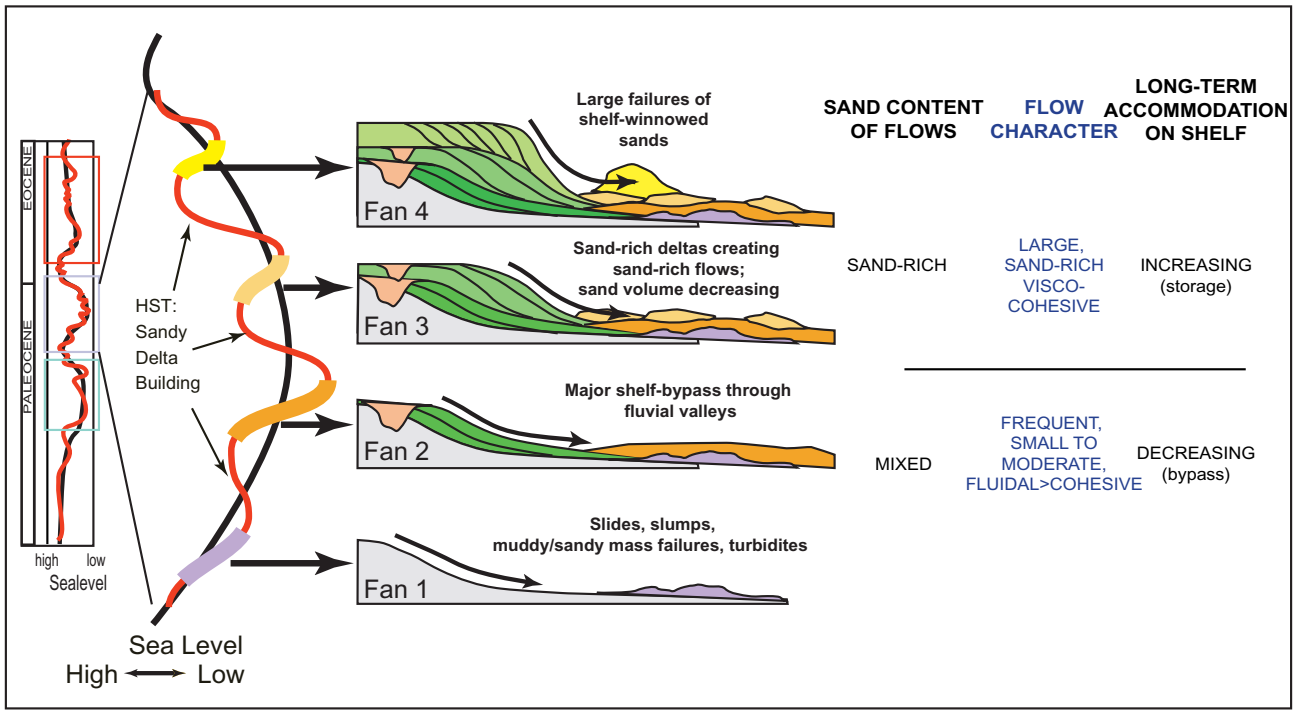

Figure 19. Evolution of the sediment delivery system and associated basin-floor depositional patterns through a low-order sea level cycle. The vertical change in reservoir character reflects a progressive change in the composition and relative volume of the sediment gravity flows being triggered at the shelf edge and then delivered into the basin. Following initial phases of mass-transported, muddy debris flows and sandy turbidity flows, sediment gravity flows become progressively sandier and are confined in discrete channels. Latest stage sequences are locally dominated by sandy debrites. These patterns record the evolution of the lowstand shelf-margin system as it becomes progressively sandier and increasingly prone to large, sand-rich failures that maintain a semi-cohesive rheology as they flow onto the basin floor. Even though the flows are sand-rich, they were smaller volumetrically because the high frequency falls were superimposed on a the rising low order sea level curve which increases the accommodation and storage of sand on the shelf.

Alternative to Previous Evolutionary Fan Models

North Sea Studies

In their excellent analysis of the Paleogene fans, Den Hartog Jager *et al.* (1993) recognized the evolutionary patterns of the Andrew, Forties, and Tay fans. They noted that soon after initiation of the fan, sediment input reached a maximum. Initial channels lacked levees and rapidly avulsed to create erratic sand percent patterns. During later stages of fan building, the total sediment input decreased due to a decreasing rate of shelf erosion and the relative mud content of the flows increased. They argued that greater mud content improved the stability of channel levees which lead to more stable channels where the aggradation of massive sand could occur. These features then turned into mounds after differential compaction. They described this evolutionary pattern as a coupling of a "Lowstand Systems Tract" for the sand-rich lower portion of the fans and a "Transgressive Systems Tract" for the phase of fan deposition marked by decreasing sand supply and increasing mud content

Our analysis is consistent with many of the observations of Den Hartog Jager *et al.* (1993). A key departure is that we recognize that the patterns occur in a mappable, step-wise fashion across high-frequency sequence boundaries. In addition, we emphasize that the character of the flows did not get muddier but sandier and had an appreciably different flow character from those that constructed the early part of the fan. Turbidites channels give way to mounded sandy debrites. No evidence of classical levees exists in the study area. The drill-well penetrations on the margin of the highly mounded geometries show little to no thin-bedded sand. These wells should be dominated by thin-bedded turbidites if constructional levels are present to help to confine the channel forms. Seismic and well data show the boundary between sandstone-rich channel forms and background shale is very abrupt. The shaley units that do overly the highly mounded bodies commonly display draping relationships, suggesting these strata are genetically unrelated and likely a post-depositional hemipelagic facies. In addition, each shale unit has been tied to major fan abandonment stages.

Contrast to the Classic Exxon Model

Posamentier *et al.* (1991) presented model for submarine fan deposition within a sequence stratigraphic framework. The lowstand systems tract was divided into two units: lowstand fan and lowstand wedge. Fans were deposited when relative sea level fell and wedges were deposited during the subsequent slow rise or stillstand.

An important implication of this model is the prediction of a decreasing sand:mud ratio during the latter part of the relative sea level lowstand. This sedimentation pattern is not consistent with the observations presented in this study of the North Sea Paleogene fans. We infer that the model presented in Posamentier *et al.* (1991) should be restricted to sediment supply systems that do not overwhelm the increasing accommodation from a rising relative sea level. That is, most of the sand-grade sediment is trapped in incised valleys during the latter stage of the lowstand to transgressive part of the cycle and is not allowed to reach the slope or basin floor. In contrast, the sediment supply for the Paleogene fan systems is sufficient to aggrade a significant shelf-edge delta system that would fail during high-frequency lowstands to provide sand-rich flows into the basin, even though low-order relative sea level is rising. The ingredients to form the predicted low sand:mud slope fan do not occur in the Paleogene system of the North Sea. Therefore, the model presented here may provide improved capabilities to predict sand percent and reservoir architecture in systems characterized by a very high sand supply that is probably tectonically driven.

Conclusions

1. Major basin-floor "fans" are sequence sets composed of mappable sequences. This is consistent with the work of Neal (1996) and Den Hartog Jager *et al.* (1993). The high quality data set of well log, biostratigraphy, and 3D seismic enable the characterization and subsequent comparison of the high-frequency building blocks.

2. High frequency sequences display progressive changes in reservoir characteristics, sand percent, architecture, and seismic geometries.

3. Changes in fan architecture and reservoir characteristics are driven by evolution in the shelf-edge sediment delivery system. As shelfal accommodation increases during the rising limb of low-order cycle, flows tend to evolve into sandier, higher quality flows that locally give rise to highly mounded geometries. This increasing sand content is occurring as overall fan size is decreasing.

4. The model aids in explaining some enigmatic geometries and prevailing sand percent characteristics of sandstone-rich basin floor fans. We also feel it provides an alternative to the classic Exxon model which predicts sand-rich basin floor successions to be capped by a relatively sand-poor slope-fan succession having leveed channels forming the reservoir facies.

Acknowledgments

We acknowledge the work of several EssoUK geoscientists who materially contributed to this project Geoffrey Fahrquharson, JanEiner Tellefsen, George Thomas, Mette Torjusen, and Robby Kilroy. Jie Huang (EMURC) has helped model the decompaction of the Tay sandstone bodies. We thank EssoMobil International Ltd., Shell UK, and ExxonMobil Upstream Research companies for the permission to publish this work. GCSEPM reviewers, Jordy Pacht, Arnold Bouma, and Gary Stephens provided many improvements to the manuscript.

References

Angevine, C.L., P.L. Heller, and C. Paola, 1990, Quantitative sedimentary basin modeling: AAPG, Tulsa, OK, Continuing Education Course Note Series #32, 133 pp.

Den Hartog Jager, M.R. Giles, and G.R. Griffiths, 1993, Evolution of Paleogene submarine fans of the North Sea in space and time, *in* J.R. Parker, (ed.), Petroleum Geology of Northwest Europe: Proceedings of the 4th Conference, Geological Society London, pp. 59-71.

Elverhøi, A., H. Norem, E.S. Anderson, J.A. Dowdeswell, I. Fossen, H. Haflidason, N.H. Kenyon, J.S. Laberg, E.L. King, H.P. Sejrup, A. Solheim, and T. Vorren, 1997, On the origin and flow behavior of submarine slides on deep-sea fans along the Norwegian-Barents Sea continental margin: Geo-Marine Letters, v.17, pp. 119-125.

Iverson, R.M., 1997, The physics of debris flows: Reviews in Geophysics, v. 35, pp. 245-296.

Major, J.J., and Iverson, R.M., 1999, Debris-flow deposition: Effects of pore-fluid pressure and friction concentrated at flow margins: Geological Society of America Bulletin, v. 111, pp. 1424-1434.

Neal, J. E., 1996, A summary of Paleogene sequence stratigraphy in northwest Europe and the North Sea, *in* R. W. Knox, R. M. Corfield, and R. E. Dunay, (eds.), Correlation of the Early Paleogene in Northwest Europe: Geological Society Special Publication No. 101, The Geological Society Publishing House, London, pp. 15-42.

Posamentier, H.W., R.D. Erskine, and R.M. Mitchum Jr., 1991, Models for submarine-fan deposition within a sequence-stratigraphic framework, *in* P. Weimer, and M.H. Link, (eds.) Seismic Facies and Sedimentary Processes of Submarine Fans and Turbidite Systems: Springer-Verlag, New York, pp. 127-136.

Shanmugam, G., Bloch, R.B., Mitchell, S.M., Beamish, G.W.J., Hodgkinson, R.J., Damuth, J.E., Straume, T., Syversten, S.E., and Shields, K.E., 1995, Basin-floor fans in the North Sea: Sequence stratigraphic models vs. sedimentary facies: AAPG Bulletin, v. 79, pp. 477-512.

Shanmugam, G., 1996, High-density turbidity currents: are they sandy debris flows?: Journal of Sedimentary Research, v. 66, p 2-10.

Shanmugam, G., 2000, 50 years of the turbidite paradigm (1950s-1990s): deep-water processes and facies models - a critical perspective: Marine and Petroleum Geology, v. 17, pp. 285-342.